

RESEARCH

Open Access



# Heme-induced lung injury in human precision cut lung slices: a new model for acute lung injury

Namrata Kewalramani<sup>1,2\*</sup>, Carlos Machahua<sup>1,2</sup>, Thomas Michael Marti<sup>3,4</sup>, Cas Zandbergen<sup>5</sup>, Savvina Chortarea<sup>5</sup>, Jessica Beretta-Piccoli<sup>5</sup>, Christophe von Garnier<sup>6</sup>, Patrick Dorn<sup>3,4</sup>, Kleanthis Fytianos<sup>5</sup> and Manuela Funke-Chambour<sup>1,2</sup>

## Abstract

**Background** Acute respiratory distress syndrome (ARDS) causes high mortality and has no specific pharmacological treatment. Scarcity of drugs against ARDS is in part due to the lack of models for ARDS. As raised serum heme levels are associated with higher mortality in patients with ARDS, we hypothesised that circulating heme contributes to ARDS pathology and can induce lung injury resembling human disease. We aimed to develop a new model for acute lung injury and ARDS research with heme-induced injury in human precision cut lung slices (PCLS).

**Methods** We analysed heme and its degrading enzymes along with inflammatory cytokines in patients with coronavirus disease 2019 (COVID-19) and ARDS compared to healthy adult subjects. In PCLS, we studied effects of heme on cell survival, membrane integrity, the transcriptome by gene expression and the proteome by protein expression analysis or ELISA. We also tested synergistical effects with lipopolysaccharide (LPS) on cell survival in addition to heme to simulate bacterial infection.

**Results** Patients with COVID-19 and ARDS had increased serum levels of heme and heme oxygenase 1 (HO-1) compared to controls. In PCLS, heme induced cell death in a dose-dependent manner, stimulated pro-inflammatory and injury signals and triggered changes to the extracellular matrix (ECM). Comparative analyses of the lung transcriptomic and proteomic signatures revealed 27 common markers (log<sub>2</sub> fold change greater than 1, at adjusted (adj) p-value < 0.05 significant), most of which were inflammatory. Similar inflammatory cytokines were raised in blood from patients with COVID-19 and ARDS compared to controls. LPS did not increase cytotoxicity in addition to heme.

**Conclusion** Heme induced inflammatory cytokine release and cell death in human PCLS, resembling the patterns observed in blood samples from patients with COVID-19 and ARDS. Thus, heme-stimulated PCLS represent a novel *ex vivo* model for mechanistic studies for acute lung injury and ARDS.

**Keywords** Acute respiratory distress syndrome, Precision cut lung slices, Heme, Transcriptomics, Proteomics, Inflammation

\*Correspondence:

Namrata Kewalramani

Namrata.kewalramani@gmail.com

Full list of author information is available at the end of the article



© The Author(s) 2025. **Open Access** This article is licensed under a Creative Commons Attribution-NonCommercial-NoDerivatives 4.0 International License, which permits any non-commercial use, sharing, distribution and reproduction in any medium or format, as long as you give appropriate credit to the original author(s) and the source, provide a link to the Creative Commons licence, and indicate if you modified the licensed material. You do not have permission under this licence to share adapted material derived from this article or parts of it. The images or other third party material in this article are included in the article's Creative Commons licence, unless indicated otherwise in a credit line to the material. If material is not included in the article's Creative Commons licence and your intended use is not permitted by statutory regulation or exceeds the permitted use, you will need to obtain permission directly from the copyright holder. To view a copy of this licence, visit <http://creativecommons.org/licenses/by-nc-nd/4.0/>.

## Background

Acute respiratory distress syndrome (ARDS) is a clinical condition of patients presenting with acute hypoxemic respiratory failure due to inflammation and acute lung injury [1]. ARDS can be induced by pulmonary or extra-pulmonary causes [2]. Pneumonia is the most common pulmonary cause, whereas sepsis is the most common extra-pulmonary cause of ARDS [3]. Pneumonia can be caused by bacterial pathogens producing endotoxin in case of gram-negative bacteria (such as LPS) or viral pathogens [4]. ARDS was induced by the initial variants of severe acute respiratory syndrome coronavirus 2 (SARS-CoV-2) virus and led to 7.1 million deaths globally [5]. Bacterial superinfection was commonly observed in patients with COVID-19 related ARDS [6]. Even outside the pandemic setting, ARDS contributes to a major healthcare burden and has a mortality of 34.9% due to mild ARDS and 46.1% due to severe ARDS [7]. The management of ARDS patients is mainly supportive using oxygen therapy while no effective pharmacological therapy is available to date [8]. The biggest challenge in developing pharmacological therapy is the heterogeneity of ARDS in terms of aetiology, pathogenesis, clinical manifestation as well as treatment response [8]. Based on plasma concentration of inflammatory cytokines such as interleukin 6 (IL-6), interleukin 8 (IL-8), tumour necrosis factor (TNF), and others [9, 10], two ARDS phenotypes have been defined: the hyper- and hypo-inflammatory ARDS phenotype. The hyper-inflammatory phenotype is associated with a higher mortality risk [9, 10]. Higher mortality was also associated with increased circulating cell-free hemoglobin (CFH) in severe sepsis patients [11].

In patients with critical illnesses such as ARDS due to sepsis, red blood cells (RBCs) are often damaged, releasing hemoglobin into the intravascular and intra-alveolar spaces [12]. Hemoglobin molecules consist of four polypeptide chain with heme embedded in each polypeptide chain [13]. Heme is composed of a ring like organic compound known as a porphyrin, to which an iron atom is attached [13]. Heme has pro-oxidant, inflammatory and cytotoxic properties [14, 15]. Shaver et al. [16] reported that the level of CFH in the airspace in ARDS correlated with increased permeability of the respiratory barrier and that the damage induced by CFH is mediated by heme. Raised levels of heme [17, 18] and its catabolites [19, 20] were found in serum or bronchoalveolar lavage (BAL) of patients with ARDS. Heme oxygenase -1 (HO-1) is a stress response protein, that catabolises heme and is induced following exposure to heme and pro-inflammatory cytokines [21]. HO-1 levels are raised in the BAL fluid and lung tissue of patients with ARDS [19]. HO-1 levels can be a useful prognostic marker in ARDS and correlate with

poor prognosis [22, 23]. Extracellular matrix (ECM) degradation in early ARDS induces the production of chemokines, cytokines, growth factors, and adhesion molecules that lead to further inflammation and injury [24].

The COVID-19 pandemic accelerated ARDS research. However, despite arduous efforts, no pharmacological treatment prevents or cures patients with COVID-19 ARDS [8, 25]. One reason for this unmet need is the limited availability of current preclinical in vitro or in vivo models of ARDS. The proinflammatory role of heme has been shown in vitro [26, 27], and elevated plasma CFH levels observed in in vivo ARDS studies further underscore its role in the disease pathogenesis [28, 29]. However, in vitro and in vivo findings can only be translated to human disease to some extent. Precision-cut lung slices (PCLS) have emerged as a powerful tool to study respiratory diseases bridging in vitro and in vivo studies [30, 31]. PCLS have preserved cellular types, original localisation within the lung scaffold and show functional responses when stimulated [32].

To address the critical knowledge gap concerning the pathophysiological role of heme in lung injury and ARDS and provide insights into the consequences of increased heme levels during ARDS, we suggest a new ex vivo model of heme-induced lung injury in human PCLS.

## Methods

### Human lung sample collection and PCLS generation

We generated PCLS from human lung tissue that was obtained from 21 patients who underwent thoracic surgery at the University Hospital (Inselspital) in Bern. Residual lung tissue from diagnostic procedures was utilized for PCLS generation. In case of cancer diagnosis, lung tissue was obtained from a tumour-free margin of a minimum of 5 cm. Patients consented to the use of residual tissue for research. Tissue sampling was approved by the local Ethics Committee, Bern, Switzerland (KEK-BE\_2018-01801, KEK-02418). The age, gender, primary diagnosis, smoking status and the test performed using PCLS of these patients are described in Table 1.

Lung tissue was processed immediately or within a maximum of 18 h after surgery. Until the processing was started the lung tissue was kept refrigerated at 4°C in complete medium containing DMEM, high glucose, GlutaMAX™ supplement, pyruvate (Gibco) containing 20mM HEPES (Sigma Aldrich) and 1% antibiotic/antimycotic 100× (Sigma Aldrich) following previously published protocols [33]. If overnight storage of lung tissue was required, ITS supplement (I3146, Sigma Aldrich) and 0.1% fetal bovine serum were added. Tissue was processed in sterile conditions. Two percent

**Table 1** Clinical information from PCLS tissue donors

Donor No	Gender	Age (years)	Diagnosis	Smoking status	Methods and analysis
1	Female	71	NET	Unknown	XTT, ELISA
2	Male	74	NSCLC, squamous	Ex-smoker, 30 PY	ELISA, transcriptomics, proteomics
3	Male	73	NSCLC, squamous	Ex-smoker, 50 PY	ELISA
4	Male	62	Lung Metastasis	Non-smoker	XTT, ELISA
5	Male	73	Lung Metastasis	Ex-smoker, 50 PY	XTT, ELISA
6	Male	62	Lung Metastasis	Non-smoker	ELISA, transcriptomics, proteomics
7	Male	62	NSCLC, adenocarcinoma	Ex-smoker, 70 PY	ELISA, transcriptomics, proteomics
8	Female	54	NSCLC	Smoker, 30 PY	XTT, ELISA, LDH, transcriptomics, proteomics
9	Male	39	Congenital pulmonary airway malformation	Unknown	XTT, ELISA, LDH, transcriptomics, proteomics
10	Female	64	NSCLC, squamous	Smoker, 40 PY	XTT, ELISA, LDH, transcriptomics, proteomics
11	Female	67	B-Cell Lymphoma	Ex-smoker, 20 PY	ELISA, LDH, transcriptomics, proteomics
12	Male	77	NSCLC, squamous	Ex-smoker, 60 PY	ELISA, LDH, transcriptomics, proteomics
13	Male	73	NSCLC, squamous	Smoker, 100 PY	LDH, immunofluorescence
14	Male	67	NSCLC, adenocarcinoma	Smoker, 50 PY	LDH
15	Female	58	NSCLC, adenocarcinoma	Ex-smoker, 100 PY	LDH
16	Male	72	NET	Ex-smoker, 100 PY	Immunofluorescence
17	Female	62	NSCLC, adenocarcinoma	Non-smoker	Immunofluorescence
18	Female	64	NSCLC, adenocarcinoma	Smoker, 50 PY	Immunofluorescence
19	Female	47	NSCLC	Non-smoker	XTT, ELISA
20	Male	78	NSCLC, adenocarcinoma	Non-smoker	XTT, ELISA
21	Female	51	Lung metastasis	Unknown	XTT, ELISA

ELISA enzyme-linked immunosorbent assay, LDH lactate dehydrogenase, NET neuroendocrine tumour, NSCLC non-small cell lung cancer, PY pack years, XTT 2,3-bis(2-methoxy-4-nitro-5-sulphophenyl)-5-carboxanilide-2H-tetrazolium

low melting point agarose (A9414, Sigma Aldrich) was used to infiltrate the lung tissue and tissue blocks were obtained. To generate PCLS, lung tissue blocks were cut at 400  $\mu\text{m}$  thickness using the Compressstome<sup>®</sup> VF 310-0Z Vibrating Microtome (Precisionary, USA). PCLS were cultured in complete medium. Before further processing, PCLS were rested in the incubator at 37 °C, 5% CO<sub>2</sub> overnight. PCLS of 4mm diameter were standardised using biopsy punches (Siramo, Switzerland) and cultured in 48-well plates (Falcon) with 250  $\mu\text{l}$  of complete medium per well. For recovery from stress induced by processing, the PCLS were rested in the incubator at 37 °C, 5% CO<sub>2</sub> for 24 h before starting the experiments.

#### Heme preparation

Heme (10mM) was prepared by dissolving 65.2 mg of Hemin (51280, Sigma Aldrich, BioXtra  $\geq$  96% HPLC) in 10 ml of 0.1 M NaOH (Merck). The pH was adjusted to pH range 7.4–7.8 with 85% phosphoric acid (49685, Sigma Aldrich). The heme solution was filtered through a 0.22  $\mu\text{m}$  (Millipore) filter under sterile conditions in our BSL2 hood. Heme was aliquoted and stored at – 20 °C and used for experiments within a week.

#### Heme stimulation

Before stimulation, PCLS were washed twice with Dulbecco's phosphate buffered saline (DPBS) (D8537, Sigma Aldrich) to remove any residual RBCs in PCLS. PCLS were stimulated without (controls) or with heme (100  $\mu\text{M}$  in 250  $\mu\text{l}$  of complete medium without fetal bovine serum) for 24 h. After incubation, supernatants were collected from each well. PCLS were washed twice with DPBS, then snap frozen and collected in separate cryovials for RNA and protein isolation or used for viable immunofluorescence staining.

#### LPS stimulation

PCLS were stimulated with LPS (tlrl-eblps, InvivoGen) alone (100 ng/ml in 250  $\mu\text{l}$  of complete medium without fetal bovine serum) or LPS combined with heme (LPS 100 ng/ml and heme 100  $\mu\text{M}$  in 250  $\mu\text{l}$  of complete medium without fetal bovine serum) for 24 h.

#### Viability and cytotoxicity assays

We determined cell viability after heme-stimulation with CyQUANT<sup>™</sup> XTT Cell Viability assays (Thermo Fisher Scientific). PCLS (1 PCLS/well in a 48 well-plate with 250  $\mu\text{l}$  of medium without FBS per well) were stimulated

with different concentrations of heme (0, 50, 100, 150, 200  $\mu$ M) for 24 h. Then, XTT reagent was added to PCLS in culture as per the manufacturer's instruction. To determine cytotoxicity, CyQUANT™ LDH Cytotoxicity fluorescence assay (Thermo Fisher) was performed using supernatants from PCLS according to the manufacturer's instruction. The protocols for the viability and cytotoxicity were adapted for the PCLS experiments. PCLS stimulated with 25  $\mu$ l of 1X lysis buffer (Invitrogen) for 45min were used as a positive control for the viability and cytotoxicity assays. Absorbance and fluorescence were measured in the "Varioskan LUX Multimode Microplate Reader" (Thermo Fisher) by subtracting the blank (supernatant alone), following the manufacturer's recommendations.

### Immunofluorescence

After 24 h of stimulation with heme, the PCLS were washed with DPBS and exposed to a far-red fluorescent dye, DRAQ7 (ab109202, Abcam, 1:250 dilution) for 10 min, revealing uptake in nonviable cells with damaged membranes. As a positive control, PCLS were stimulated with 1X lysis buffer (Invitrogen) for 45 min. The PCLS were then stained with diamidino-2-phenylindole (DAPI, Sigma-Aldrich) for 5 min as a counterstain for nuclei. PCLS were mounted on slides with mounting medium EMS Shield Mount with DABCO™. Images were taken in the CellVoyager™ CQ1 Benchtop High-Content Analysis System within 15 min. All pictures were taken with the same 2 $\times$  magnification, exposure and intensity. Images were processed with ImageJ (version 2.14, Java 1.8, LOCI, University of Wisconsin).

### Transcriptome analysis

Total RNA was isolated for bulk RNA-sequencing using PCLS from 7 donors. We used the proposed combination TRIzol® (A33250, Thermo Fisher) and RNeasy Micro Kit (Qiagen) for RNA isolation according to Stegmayr et al. [34]. The quality control and sequencing were performed at the Next Generation Sequencing Platform of the University of Bern. The quantity and quality of the purified total RNA were assessed using a Thermo Fisher Scientific Qubit 4.0 fluorometer with the Qubit RNA BR & HS Assay Kit (Thermo Fisher Scientific) and a Fragment Analyzer RNA Kit (Agilent). Sequencing libraries were made with 355 ng input RNA using an Illumina TruSeq Stranded mRNA Library Prep kit (Illumina) in combination with TruSeq RNA UD Indexes (Illumina) according to Illumina's guidelines. The resulting cDNA libraries were evaluated using a Thermo Fisher Scientific Qubit 4.0 fluorometer with the Qubit dsDNA HS assay Kit (Thermo Fisher Scientific) and an Agilent Fragment Analyzer (Agilent) with a HS

NGS Fragment Kit (Agilent), respectively. Pooled cDNA libraries were sequenced paired-end using a NextSeq 1000/2000 P2 Reagents (100 Cycles) v3 (Illumina) on an Illumina NextSeq 1000 instrument. The run produced on average, 32.7 million reads/library.

Data analysis was supported by the "Interfaculty Bioinformatics Unit (IBU) and Swiss Institute of Bioinformatics (SIB), University of Bern, Bern, Switzerland". The quality of the RNA-seq data was assessed using FASTQC v.0.11.9 [35] and RSeQC v.4.0.0 [36]. The reads were mapped to the reference genome using HiSat2 v.2.2.1 [37]. FeatureCounts v.2.0.1 [38] was used to count the number of reads overlapping with each gene as specified in the genome annotation (Homo\_sapiens.GRCh38.107). The Bioconductor package DESeq2 v1.38.3 [39] was used to test for differentially expressed genes (DEG) between the experimental groups. ClusterProfiler v4.7.1 [40] was employed to identify gene ontology (GO) terms containing unusually many differentially expressed genes. Gene set enrichment analysis (GSEA) [41] was run in ClusterProfiler v4.7.1 [40] using gene sets from the Kyoto Encyclopedia of Genes and Genomes (KEGG) [42]. All analyses were run in R version 4.2.1 (2022-06-23) (R Core Team 2022). Data exploration and visualisation was done using the Shiny application v1.6.0 [43]. Log2 fold change (FC) greater than 1, at adj p-value < 0.05 was considered significant.

### Proteome analysis of protein lysates

Total protein was isolated using PCLS from 7 donors used for transcriptome analysis. Protein was extracted using radioimmunoprecipitation assay (RIPA) lysis buffer (89900, Thermo Fisher), protease inhibitor cocktail (Sigma Aldrich) and phosphatase inhibitor cocktail 1 (Sigma Aldrich) following the methods as previously described [33]. Further processing of samples was performed at the Core Facility Proteomics & Mass Spectrometry of the University of Bern. Samples were precipitated with 5-volume acetone at -20 °C for 4 h. The pellets were re-suspended in 8M urea/50mM Tris pH8 and protein concentration was determined with Qubit Protein Assay (Invitrogen). An aliquot corresponding to 5  $\mu$ g of protein was reduced, alkylated, and digested with LysC for 2 h at 37 °C, followed by Trypsin at room temperature overnight. The digests were analyzed by nano-liquid chromatography on a Dionex, Ultimate 3000, (ThermoFischer Scientific) coupled to a timsTOF Pro (Bruker Daltonics) which generated data in data dependant acquisition (DDA).

Data analysis was performed at the Core Facility Proteomics & Mass Spectrometry of the University of Bern. The DDA data were used to produce a spectral library with fragpipe [44] version 20.0 with the

following parameters: human database from SwissProt [45]. Differential expression tests were performed with the moderated paired t-test; for multiple test correction, the R tool *fdrtool* [46] was applied to generate differentially expressed protein (DEP) in between the experimental groups. Significance criteria using 20 imputation cycles were applied as described in Uldry et al. [47], imposing a minimum log<sub>2</sub> FC of 1 in absolute value, and a maximum adj p-value of 0.05. The t-statistic was then used as a ranking metric for gene set enrichment analysis with the R tool *ClusterProfiler* [40] and the KEGG pathway database [42].

We used the Perseus platform v1.6.14.0 (Max Planck Institute of Biochemistry, Germany) to compare the list of DEG to the DEP to find common markers [48]. We used the search tool for the retrieval of interacting genes/proteins (STRING) data base version 12 (Global Biodata Coalition and ELIXIR) to understand the function and role of DEG and DEP in our model (<https://string-db.org/>) [49].

#### Cytokine measurements

IL-6 and IL-8 ELISA kits (Bio-Techne) were used to test their levels in supernatants from PCLS (in triplicate) according to the manufacturer's instructions. Plates were read in a "Varioskan LUX Multimode Microplate Reader" (Thermo Fisher).

#### Serum samples from COVID-19 ARDS patients and healthy individuals

We collected 20 serum samples from patients admitted to a hospital in Switzerland due to SARS-CoV-2 between June 2020 and September 2021. The blood samples were collected within 7 days of admission and stored at the Bio-Bank at Inselspital, University Hospital Bern (n=7) or at the Bio-Bank at CHUV, Lausanne University Hospital (n=13). All 20 patients with COVID-19 were admitted due to respiratory reasons and ARDS [1]. The participants signed a consent form before inclusion in the study that was approved by the local ethical committee (KEK 2020-00799). For comparison, 20 serum samples from healthy adults were collected. The age group of the healthy adult group was above 40 years, similar to the age group in the patient group. Blood was collected from 10 healthy volunteers from the Pulmonology Department at Inselspital, University Hospital Bern (Swiss ethical committee Bern approval KEK\_246/15 PB\_2016-01524). 10 healthy serum samples were purchased from a biospecimen collection company (SanguineBio, Woburn, MA, USA).

#### Human serum analysis

The heme assay kit (Abcam, ab272534) was used for determining heme concentration in the serum samples with a dilution of 1:5, following manufacturer's recommendations. Undiluted human serum samples were analyzed by ProcartaPlex Luminex (Thermo Fisher) customized multiplex kits (PPX-12-MXGZHHG and PPX-02-MXH6C3E).

#### Statistical analysis

Results are expressed in mean ± standard deviation for all continuous variables. GraphPad Prism (version 9) was used for statistical analysis. Statistical analysis for HO-1 was performed by unpaired t-test whereas for heme, and multiplex it was performed by Mann–Whitney test and Benjamini–Hochberg correction for multiple testing was applied. For the XTT assay with different concentration of heme, one way ANOVA, and Tukeys multiple comparison test as post-hoc test was performed. For LDH assay and ELISAs, Wilcoxon test was performed. For XTT assay and IL-6 ELISA comparing effects of heme and combination of heme and LPS, one way ANOVA and Dunn's multiple comparisons test was performed. P-value < 0.05 was considered significant. We used "Cytokines and Inflammatory Response (*Homo sapiens*)" from WikiPathways database [50] to match our results (<https://www.wikipathways.org/pathways/WP530.html>).

## Results

### Heme increases cytotoxicity and reduces cell survival in human PCLS

Compared with the control group (n=20), serum heme levels in patients with COVID-19 and ARDS (n=15) were significantly increased (p=0.002; 35.02 ± 16.5 vs 46.6 ± 18.3 μM, respectively, Fig. 1a), indicating heme accumulation. Serum HO-1 levels were nearly twice as high in patients with COVID-19 and ARDS compared to healthy adults (p=0.007; 3.17 vs 1.59 ng/ml, respectively, Fig. 1b). Furthermore, serum ferritin levels were raised in patients with COVID-19 and ARDS compared to healthy adults (p=0.001; 56.26 ng/ml vs 5.59 ng/ml, respectively, Fig. 1c). In the next step, we evaluated the direct effects of heme on lung tissue in the in our ex vivo model and stimulated human PCLS with different heme concentrations for 24 h. Our results demonstrated a dose-dependent decrease in PCLS viability with a 30% reduction at 50 μM and a 85% reduction at 200 μM, as measured by XTT (Fig. 1d). The following experiments were performed at a concentration of 100 μM or IC<sub>50</sub>. Cytotoxicity, as measured by LDH assay (Fig. 1e), was raised by a median of 66% in the PCLS stimulated with 100 μM heme compared to controls. In addition, the heme-stimulated

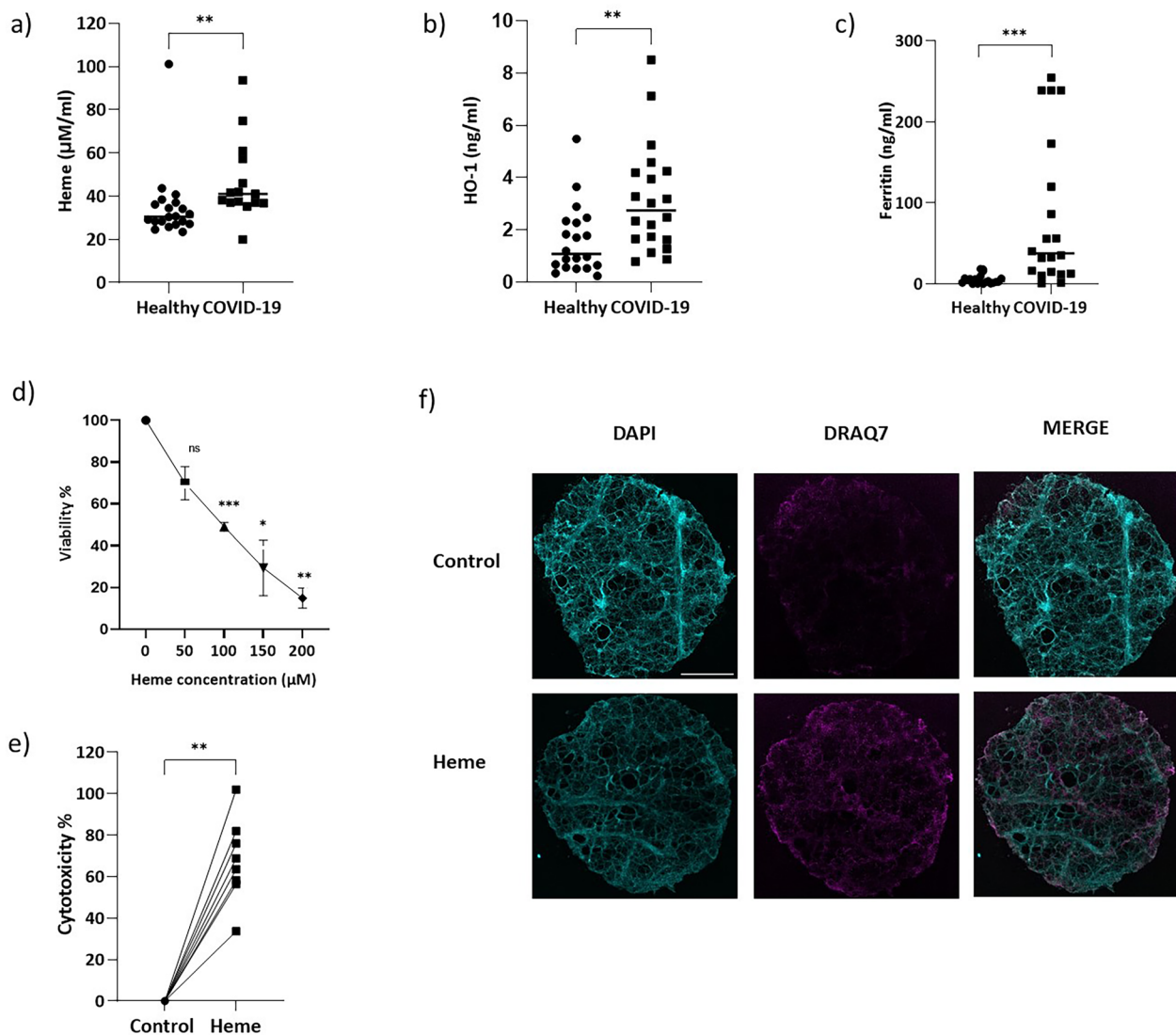


**Fig. 1** Heme affects cytotoxicity and cell survival in PCLS. **a** Heme levels measured by colorimetric heme assay were raised in serum of patients with COVID-19 and ARDS ( $n = 15$ ) as compared to healthy controls ( $n = 20$ ,  $p = 0.002$ ). **b** HO-1 levels measured by ELISA were greater in serum of patients with COVID-19 ( $n = 20$ ) compared to healthy controls ( $n = 20$ ,  $p = 0.007$ ). **c** Ferritin levels were raised in serum of patients with COVID-19 and ARDS ( $n = 20$ ) as compared to healthy controls ( $n = 20$ ,  $p = 0.001$ ). **d** XTT assay showed heme reduces the viability of PCLS up to 50% at 100  $\mu\text{M}$  ( $n = 3$ ,  $p = 0.0003$ ). Results are displayed as mean  $\pm$  SD. (\* $p < 0.05$ , \*\* $p < 0.01$ , \*\*\* $p < 0.001$ ). **e** Cytotoxicity % as measured by LDH assay after treatment with 100  $\mu\text{M}$  heme ( $n = 8$ ,  $p = 0.0078$ ). **f** Qualitative representative immunofluorescence images of DRAQ7 (magenta), in human PCLS stimulated with heme ( $n = 3$ ) and medium alone (control). Nuclei were stained with DAPI (cyan). Pictures acquired at 2X magnification. Scale bar = 1 mm

PCLS had a significant uptake of the nuclear dye DRAQ7 (Fig. 1f) as compared to the control PCLS, confirming that cell membranes were compromised and the cells nonviable. PCLS treated with lysis buffer was used as positive control (Supplemental Fig. S1).

#### Heme induces pro-inflammatory and injury signals in PCLS

Principal component analysis (PCA) based on the 500 most variable genes revealed the overall similarity of the gene expression profiles with or without heme in the

transcriptomic analysis (RNA-seq assay). Supplemental Fig. S2a demonstrated a separation of the heme-stimulated PCLS from the control group ( $n = 7$ ), with PC1 and PC2 explaining 59.4% of the variance. The DGE analysis revealed 1827 differentially expressed genes in heme vs control condition (Supplemental table S1), 1095 genes were downregulated, whereas 732 genes were upregulated, as displayed in the volcano plot (Fig. 2a). The 10 genes related to inflammation and ECM were clustered in a heat map (Fig. 2b), identifying *HMOX1* (HO-1 gene),

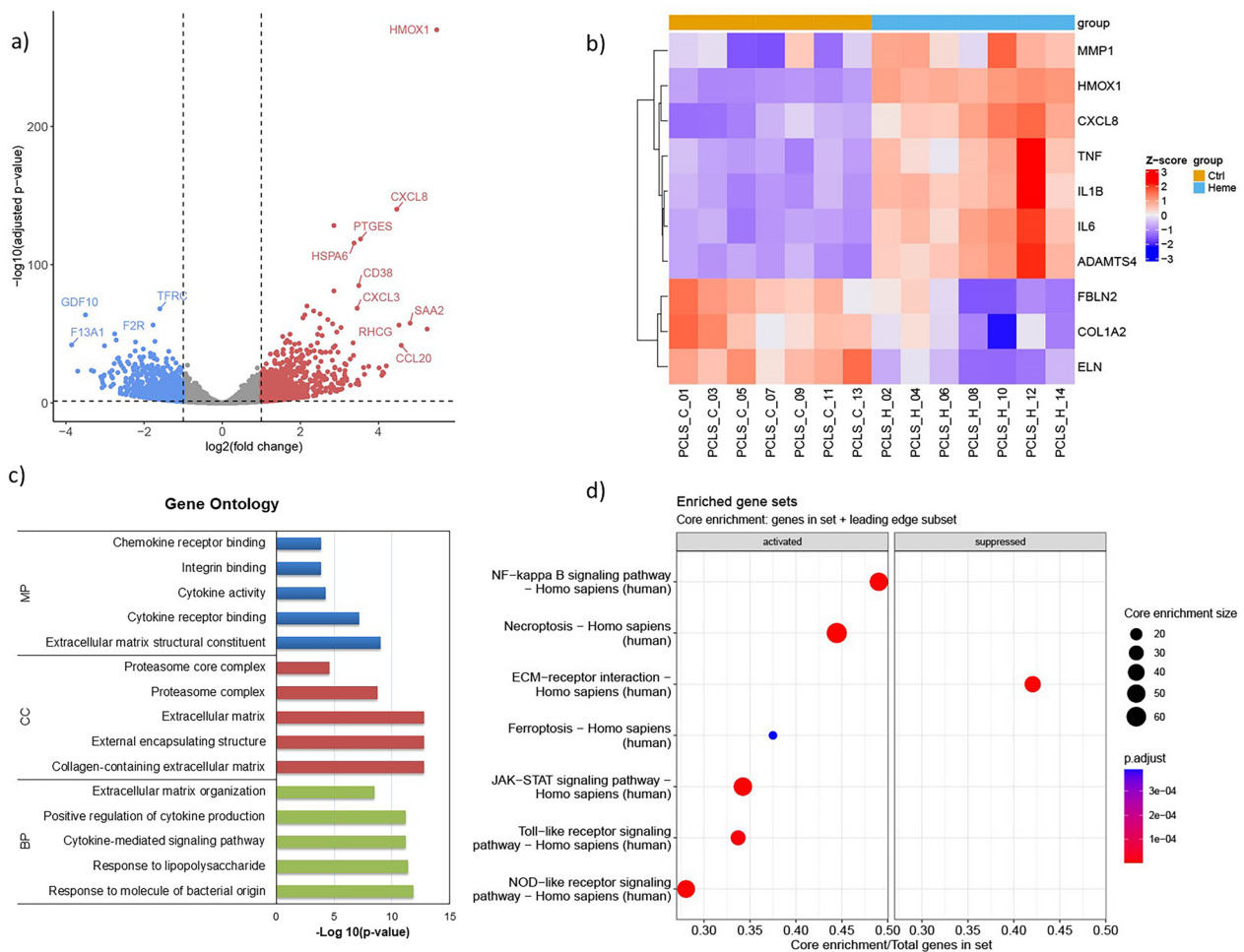


**Fig. 2** Transcriptomic profiles in heme and control PCLS. **a** Volcano plot of overall DEG between the heme-stimulated group and the control group. A total of 1827 genes were selected following  $\log_2 \text{FC} > 1$  and  $\text{adj p-value} < 0.05$ . **b** Clustered heatmap of 10 genes associated with inflammatory pathway and ECM. **c** Gene ontology overrepresentation analysis (GO ORA) of biological processes (BP), molecular functions (MF) or cellular components (CC) in heme-stimulated group compared to control ( $\text{adj p-value} < 0.05$ ) and horizontal axis corresponds to the negative log (base 10) of the p values. **d** Dot plot of activated and suppressed pathways in gene set enrichment analysis (GSEA) using KEGG database in the heme-stimulated group as compared to control group ( $\text{adj p-value} < 0.05$ ). The x-axis represents the number of genes in the core enrichment set divided by the total number of genes in the set. The size of the dots represents the size of the core enrichment set

a rate-limiting enzyme for heme degradation, as the most upregulated gene. Inflammatory genes such as *IL6* (Interleukin-6 gene), *TNF* (Tumour necrosis factor gene), *CXCL8* (Interleukin-8 gene), and *IL-1 $\beta$*  (Interleukin-1 beta gene) were also upregulated following stimulation. Proteinases such as *MMP1* (Matrix metalloproteinase 1 gene) and *ADAMTS4* (A disintegrin and metalloproteinase with thrombospondin motifs 4 gene) involved in ECM remodelling and repair were upregulated, while structural components of ECM e.g. *ELN* (Elastin gene), *FBLN1* (Fibulin 1 gene) and *COL1A2* (Collagen Type I Alpha 2 Chain) were downregulated after heme exposure. Gene ontology (GO) analyses of the five most relevant functions (Fig. 2c) highlighted that in molecular

processes (MP) differential genes in heme-stimulated PCLS belong to ECM structural constituent, whereas biological processes (BP) involved cytokine signal induction in response to external stimulus or antigen as relevant mechanisms. Meanwhile, the cellular component (CC) analysis associated the differential genes with changes in the ECM and in the proteasome complex. A complete GSEA was performed to evaluate molecular interaction according to the KEGG PATHWAY Database (Fig. 2d). Results showed activation of inflammatory pathways such as nuclear factor  $\kappa$  B (NF- $\kappa$  B) (Net enrichment score (NES)=2.35,  $p=2.10 \times 10^{-09}$ ), JAK/STAT (NES=2.08,  $p=6.47 \times 10^{-07}$ ) and toll-like receptor (TLR) signalling pathway (NES=2.04,  $p=7.45 \times 10^{-06}$ ).

Also, there was activation of two pathways of cell death-necroptosis (NES=2.17,  $p=1.96 \times 10^{-07}$ ) and ferroptosis (NES=1.66,  $p=0.0001$ ). On the contrary, ECM receptor interaction pathways were suppressed (NES=- 2.25,  $p=1.48 \times 10^{-08}$ ).

Whole proteomic profile was analysed in heme-stimulated and control PCLS. Principal component analysis (PCA) showed separation between the heme-stimulated and control group (n=7, Supplemental Fig. S2b). The proteomic analysis revealed 35 differentially expressed proteins, represented in the volcano plot (Fig. 3a, Supplemental table S2); with most of them (34 proteins) being upregulated. Inflammatory cytokines such as IL-8, CXCL1, CXCL2 and HMOX1 were the most upregulated proteins, while the coagulation factor F13A1 was the only downregulated protein. In line with our transcriptomics analysis, GSEA (Fig. 3b) of our proteomic data indicated activation of inflammatory pathways, including

NF- $\kappa$  B (NES=2.4,  $p=1.25 \times 10^{-07}$ ) and TLR (NES=2.24,  $p=0.0001$ ) signalling.

Additionally, necroptosis (NES=1.96,  $p=0.0008$ ) and ferroptosis (NES=2.05,  $p=0.001$ ) pathways were activated, consistent with the transcriptomic GSEA analysis. The activation of these inflammatory pathways was confirmed in PCLS supernatants by ELISA, which showed greater secretion of inflammatory cytokines such as IL-8 and IL-6 in PCLS after heme-stimulation ( $p=0.001$ , n=12, Fig. 3c, d). The addition of LPS to heme did not worsen the viability (n=3,  $p=0.99$ , Fig. 3e) as compared to the viability of heme stimulation. Similarly, addition of LPS to heme did not induce a statistically significant change of IL-6 as measured by ELISA (n=3,  $p=0.99$ , Fig. 3f). In the PCLS model 27 markers were identified simultaneously at the gene level and protein levels and are listed in Table 2. These markers had a positive and strong correlation in their transcriptomic and proteomic

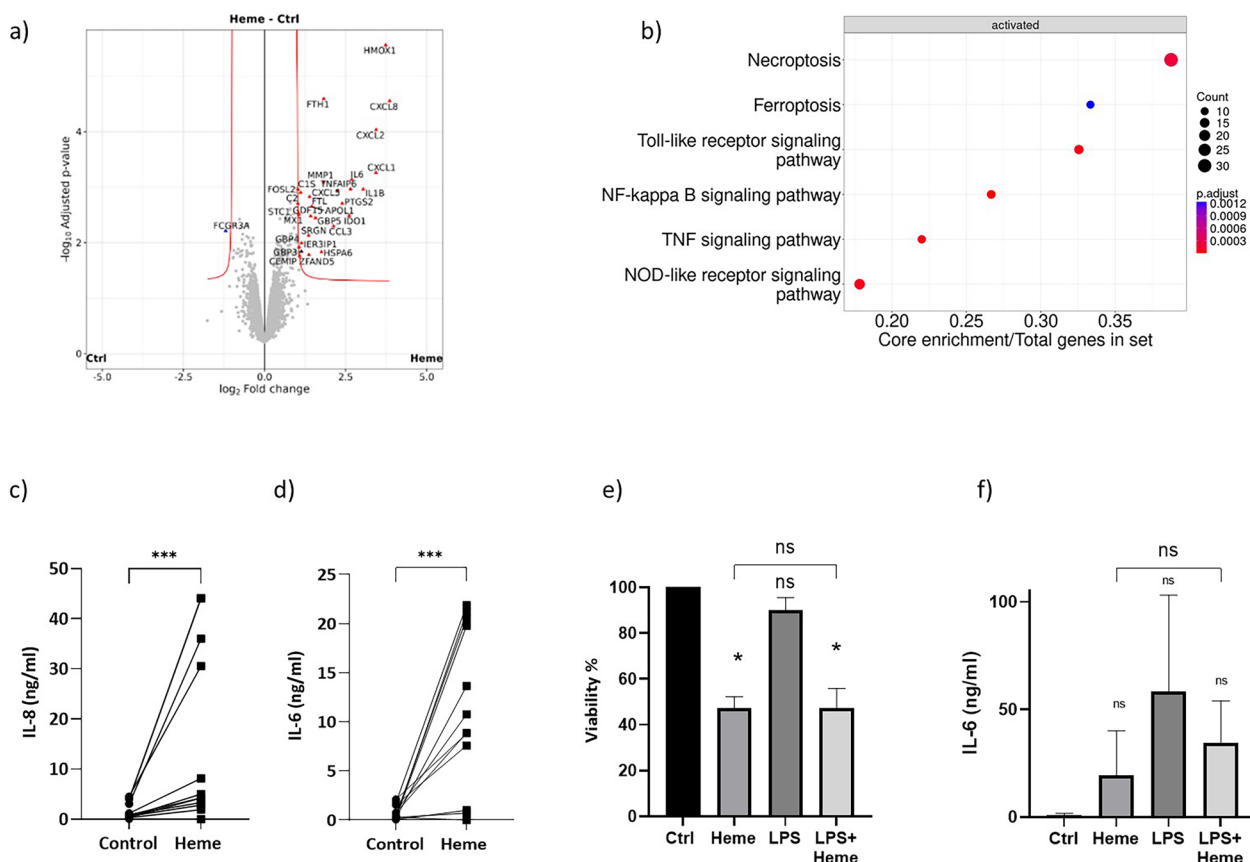


**Fig. 3** Proteomic profiles in heme and control PCLS. **a** Volcano plot of overall differentially expressed proteins (DEP) of heme-stimulated vs control group. The x-axis corresponds to the log (base 2) of the fold change and y-axis corresponds to the negative log (base 10) of the p values. Thirty-five proteins were dysregulated in heme-stimulated PCLS compared to control, following  $\log_2 FC > 1$  and  $\text{adj } p\text{-value} < 0.05$ . **b** Dot plot of activated pathways in GSEA using KEGG database in the heme-stimulated group as compared to control group ( $\text{adj } p\text{-value} < 0.05$ ). There were no suppressed pathways. **c, d** ELISA for IL-6 and IL-8 measured from supernatants, (n= 12, \*\*\* $p < 0.001$ ). **e** XTT assay did not show difference in viability in the heme and combined heme and LPS group (n=3,  $p=0.99$ ). Results are displayed as mean  $\pm$  SD (\* $p < 0.05$ ). **f** IL-6 levels measured in the heme and combined heme and LPS group (n=3,  $p=0.99$ ) did not show statistically significant difference. Results are displayed as mean  $\pm$  SD

**Table 2** Markers commonly expressed in transcriptome and proteome analysis of PCLS

Gene	Description	Transcriptomics		Proteomics		
		Log fold change	FDR	Log fold change	FDR	
1	HMOX1	Heme oxygenase 1	5.49	1.12E-270	3.73	2.77E-06
2	CXCL8	Interleukin-8	4.47	7.42E-141	3.86	2.81E-05
3	IL6	Interleukin-6	4.01	4.91E-26	2.69	0.001
4	IL1B	Interleukin-1 beta	3.75	3.82E-27	3.04	0.001
5	GBP5	Guanylate-binding protein 5	3.62	2.71E-26	1.57	0.004
6	IDO1	Indoleamine 2,3-dioxygenase 1	3.50	7.12E-14	2.61	0.003
7	HSPA6	Heat shock protein family A Member 6	3.37	2.30E-116	1.76	0.014
8	CXCL1	Chemokine (C-X-C motif) ligand 1	3.13	4.23E-29	3.43	0.001
9	PTGS2	Prostaglandin G synthase 2	3.09	2.67E-119	2.39	0.002
10	CXCL2	Chemokine (C-X-C motif) ligand 2	3.04	2.95E-55	3.44	9.25E-05
11	TNFAIP6	Tumour necrosis factor-inducible gene 6 protein	2.89	6.87E-18	2.65	0.001
12	GBP4	Guanylate-binding protein 4	2.87	1.09E-18	1.14	0.010
13	CFB	Complement factor B	2.70	4.94E-61	1.06	0.015
14	CXCL5	Chemokine (C-X-C motif) ligand 5	2.44	3.25E-19	2.26	0.001
15	FTH1	Ferritin heavy chain	2.11	2.10E-64	1.82	2.56E-05
16	CCL3	Chemokine (C-C motif) ligand 3	2.10	1.06E-06	2.13	0.005
17	ADAMTS4	A disintegrin and metalloproteinase with thrombospondin motifs 4	2.08	1.58E-22	1.04	0.013
18	MX1	MX Dynamin Like GTPase 1	2.07	2.71E-28	1.05	0.003
19	APOL1	Apolipoprotein L1	1.78	3.34E-37	1.45	0.002
20	CEMIP	Cell migration-inducing and hyaluronan-binding protein	1.67	1.62E-16	1.08	0.017
21	SRGN	Serglycin	1.65	2.16E-27	1.36	0.007
22	GDF15	Growth differentiation factor 15	1.55	8.89E-24	1.42	0.003
23	MMP1	Matrix Metalloproteinase 1	1.53	2.85E-20	1.82	0.001
24	C1S	Complement C1s subcomponent	1.34	3.88E-31	1.11	0.001
25	GBP3	Guanylate-binding protein 3	1.33	1.86E-11	1.06	0.011
26	FOSL2	Fos-related antigen 2	1.11	1.32E-15	1.03	0.001
27	FCGR3A	Low affinity immunoglobulin gamma Fc region receptor III-A	-2.05	5.14E-24	-1.20	0.006

FDR false discovery rate

expression (Spearman  $r=0.78$ ,  $p<0.0001$ , Supplemental Fig. S3).

Confirming the clinical relevance of our model findings, we detected increased levels of IL-6, IL-8, C-X-C Motif Chemokine Ligand 1 and 2 (CXCL1 and 2) and growth differentiation factor-15 (GDF-15) in the sera of patients with COVID-19 and ARDS compared with those of healthy adults (Table 3). The levels of Chemokine (CC motif) ligand 3 (CCL3), matrix metalloproteinase-1 (MMP-1), indoleamine 2,3-dioxygenase (IDO), C-X-C Motif Chemokine Ligand 5 (CXCL5) and heat shock protein 70 (HSP70) revealed no difference between healthy adults and COVID-19 patients. Figure 4a, b show scatter plots for IL-6 ( $p=0.001$ ) and IL-8 ( $p=0.023$ ) analysis respectively, demonstrating significantly increased inflammation in patients with COVID-19 and ARDS. Additionally, the scatter plot shows raised

CXCL1, CXCL2 and GDF-15 in patients with COVID-19 (Fig. 4c–e).

To summarise our findings, Fig. 5 was generated with WikiPathways [50] by using the pathway “Cytokines and Inflammatory Response (Homo sapiens)”. All the genes and proteins that matched this pathway were upregulated. Upregulated markers following heme stimulation in PCLS were mainly linked to macrophages. Macrophages activate immune cells such as T cells, neutrophils and other lung cells such as the endothelial cells and fibroblasts, for the inflammatory response via IL-6, IL-8, TNE, IL-1 $\beta$ , CXCL1 and CXCL2 that were increased in our model [24, 51, 52]. The picture integrates our results into the mechanism of possible immune cell activation and the response from structural cellular components of PCLS that drives an inflammatory response, in our case, provoked by heme itself or indirectly by lung injury induced by heme.

**Table 3** Multiplex analysis of blood from healthy adults and SARS-CoV-2 infected patients

	Name	Serum mean (pg/ml)		Adj p-value
		Healthy	SARS-CoV-2	
1	IL-6	0.0	117.5 ± 330.9	0.001
2	IL-8	0.62 ± 0.97	9.9 ± 9.2	0.023
3	CXCL1	7.64 ± 4.7	25.17 ± 25	0.001
4	CXCL2	4.94 ± 2.9	14.7 ± 16.6	0.001
5	Ferritin	5591 ± 5771	56,260 ± 68,519	0.001
6	GDF-15	237.7 ± 191.3	1365 ± 1598	0.001
7	CCL3	7.18 ± 9.5	9.5 ± 8.7	0.159
8	HSP70	99.85 ± 189.1	170.04 ± 300	0.360
9	MMP-1	668.7 ± 531.3	839.3 ± 650.6	0.456
10	IDO	18.68 ± 26.4	41.78 ± 62.6	0.560
11	CXCL5	142.2 ± 111.7	181.37 ± 223.7	0.910

Results are displayed in mean ± SD.

*CXCL1* C-X-C Motif Chemokine Ligand 1, *CXCL2* C-X-C Motif Chemokine Ligand 2, *CCL3* C-C Motif Chemokine Ligand 3, *CXCL5* C-X-C Motif Chemokine Ligand 5, *GDF-15* Growth differentiation factor-15, *IDO* Indoleamine 2,3-dioxygenase, *MMP-1* Matrix metalloproteinase-1, *HSP70* Heat shock protein-70

## Discussion

Here, we describe a new model of ALI in human PCLS triggered by heme. Using a combined transcriptomic

and proteomic approach, we investigated the effects of heme-induced lung injury ex vivo. Our study suggests that cell injury, cell death, strong cytokine stimulation, upregulation of inflammatory pathways and downregulation of ECM-receptor interaction occur in heme-stimulated PCLS. Our model findings are consistent with analyses from sera of patients with COVID-19 and ARDS, confirming their clinical relevance.

Our clinical findings in patient sera congruent with previous findings on heme and HO-1 in patients with COVID-19 related ARDS [17, 53]. In patients with ARDS, raised levels of ferritin have been previously reported [54] and may have prognostic potential [55, 56]. While heme is probably not the initial and single cause for ARDS development, raised levels in serum of patients suggest that heme might potentially contribute to lung injury and associated mechanisms. We thus investigated direct effects of heme on lung tissue in the PCLS model to evaluate its effects and simulate ex vivo some of the ARDS features.

We showed that heme induces cytotoxicity and reduces cell viability by compromising cell membrane integrity [57, 58]. Our findings are consistent with those of Ryter et al. [59] who reported that heme treatment

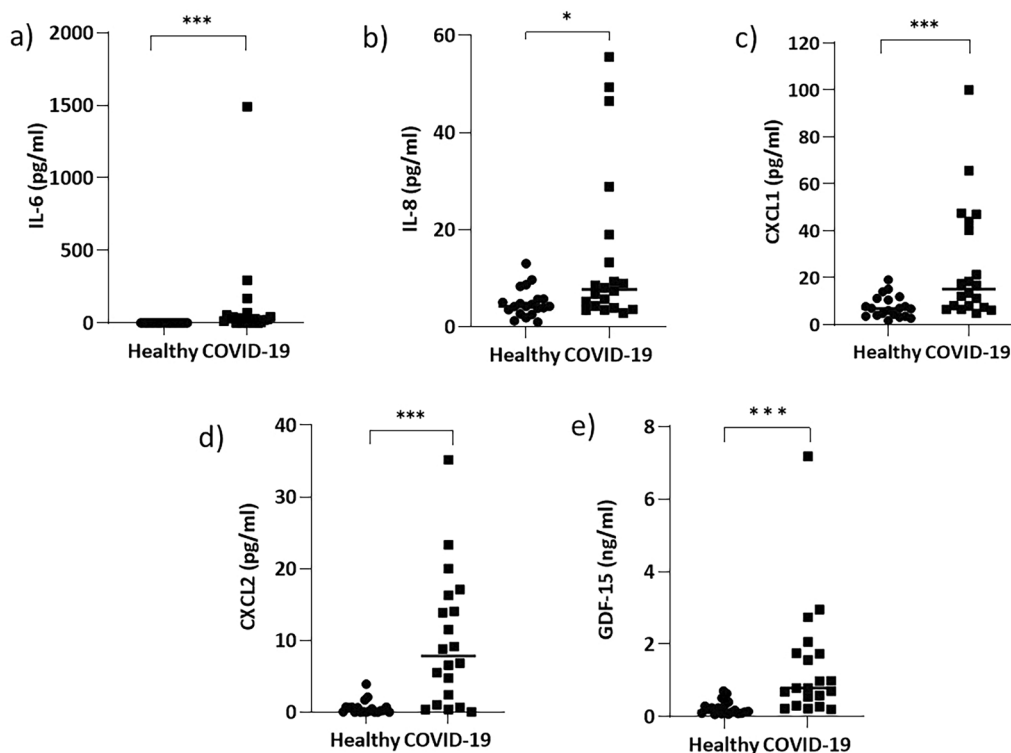


**Fig. 4** COVID-19 patients had raised inflammatory markers. **a–e** Inflammatory markers such as IL-6, IL-8, CXCL1, CXCL2 and GDF-15, respectively measured by multiplex analysis were raised in serum of patients with COVID-19 and ARDS (n = 20) as compared to healthy serum (n = 20) (\*p < 0.05, \*\*p < 0.01, \*\*\*p < 0.001)

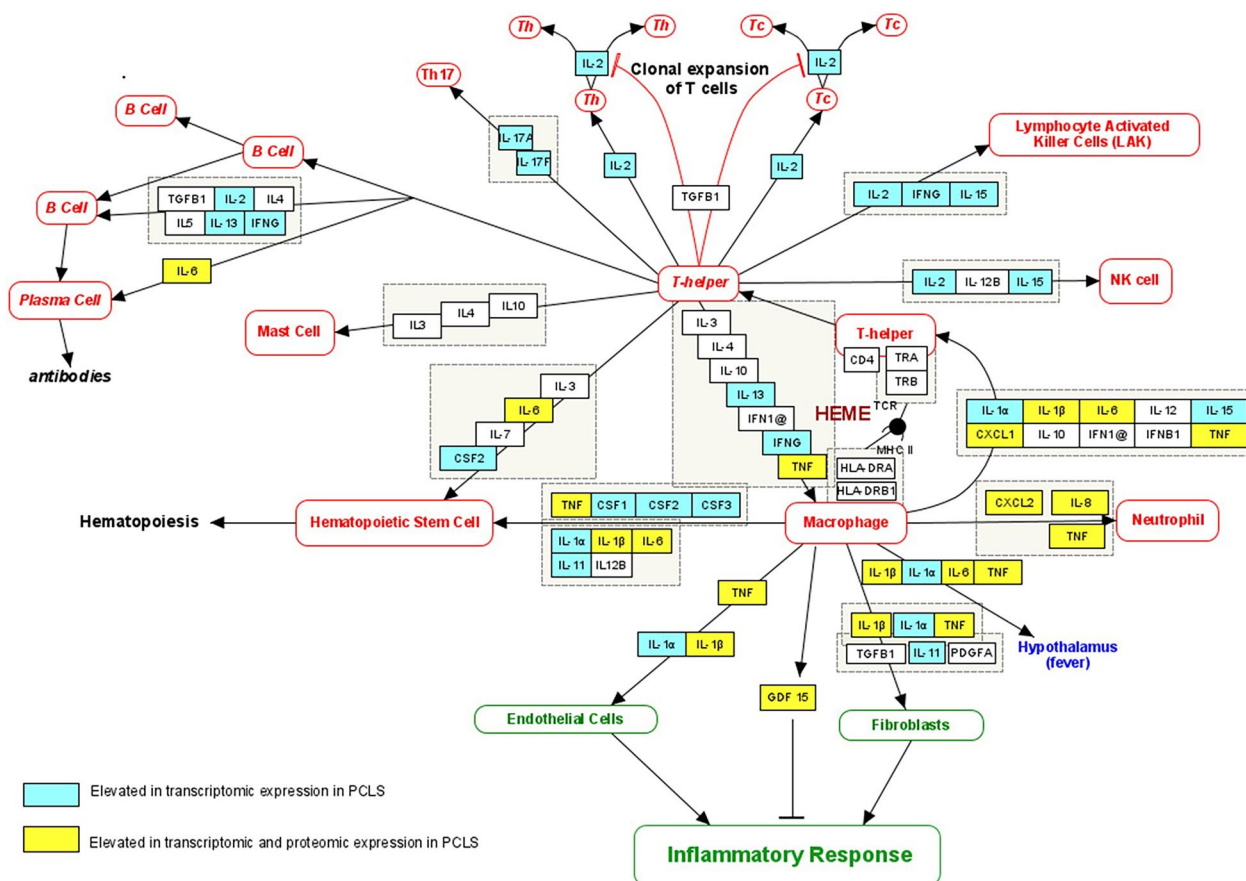


**Fig. 5** Cytokines and inflammation response from WikiPathways. 19 upregulated markers only at gene level are coloured in blue and 7 upregulated markers upregulated at the gene and protein levels are coloured in yellow. Abbreviations: CXCL1/2/8, C-X-C Motif Chemokine Ligand 1/2/8; CSF1/2/3, Colony stimulating factor 1/2/3; IFNG, Interferon gamma; GDF 15, Growth differentiation factor 15; IL-1α/1β/2/6/8/11/13/15/17A/17F, Interleukin-1α/1β/2/6/8/11/13/15/17A/17F; TNF, Tumour necrosis factor

compromises cell membrane integrity in vitro. Our enrichment analysis revealed the activation of non-apoptotic mechanism of cell death, such as ferroptosis and necroptosis, while we did not find upregulation of caspases or other markers of the classical apoptotic cell death pathways. We visualised compromised cell membrane integrity in heme-stimulated PCLS which supports the role of non-apoptotic cell death in our results. Recently the roles of necroptosis [60] and ferroptosis [61] in ARDS have received increased attention. A study on macrophages showed that heme caused early macrophage death characterized by the loss of plasma membrane integrity and morphologic features resembling necrosis [62]. The authors demonstrated that free heme causes necroptosis in macrophages by TLR4 dependant activation of NF-κ B. Correspondingly, a study using the lungs of 7 ARDS patients after autopsy found evidence of cell death by necroptosis in lung epithelial cells [60]. Conversely, Qui et al. [61] demonstrated a role of ferroptosis in the pathogenesis of

COVID-19, identifying markers of lipid peroxidation by immunostaining and lipidomics in post-mortem lungs from COVID-19 patients [61]. In heme-induced model of injury it is perceivable to expect ferroptosis. Indeed, it has been shown before that heme released by hemolysis of erythrocytes induced ferroptosis in intestinal epithelial cells in in vitro mouse model [63]. However, this has not been further investigated. Future studies using cell rescue by inhibitors of ferroptosis might help elucidate the underlying mechanisms and identify potential drug targets.

The relationship between cell death and heme-induced inflammation has been convincingly established by the work of Dutra et al. [14] and Erdei et al. [27], who demonstrated that heme stimulation caused NOD like receptor protein 3 (NLRP3) inflammasome activation dependant IL-1β production. Cytokines, such as IL-1β activate NF-κ B pathway [64]. NF-κ B plays a vital role in the inflammatory response, hence it is considered as a master regulator of inflammation by secreting

inflammatory cytokines such as TNF, IL-6, IL-8 and IL-1 $\beta$  [64]. Heme induced cell injury via necrosis is the starting point of causing inflammation caused by NLRP3 induced IL-1 $\beta$  secretion. Necrosis is a prerequisite for NLRP3 activation [65, 66]. This is in line with the findings of Li et al. [67], who reported that only necrosis causes activation of inflammation and not apoptosis. Inflammation observed after heme stimulation in PCLS supports our theory of the non-apoptotic cell death pathway being dominant in our experimental findings.

Heme reduced viability followed by increased inflammatory signals, while the observed effects might be partially due to injury itself and not specific for heme. Heme binds to TLR4 [68, 69], and TLR4 receptor binding might contribute to increased inflammatory signals. In unpublished data we observed that heme induced inflammation was not exclusively mediated by TLR4, as its inhibition did not abrogate the effects observed in our experiments. It remains unclear if other receptors are involved in the observed heme induced effects or such effects are unspecific responses to injury. The GSEA analysis revealed activation of TLR and nucleotide-binding, and oligomerization domain (NOD) signalling in the heme-stimulated PCLS confirming that in the PCLS model, heme induces inflammation via TLR4 [68, 69] and NLRP3 [14, 27]. NF- $\kappa$  B pathway has been identified as an activated pathway in the transcriptomic and proteomic analysis. Previous studies have shown, in patients with ARDS that NF- $\kappa$  B signalling pathway and JAK-STAT signalling pathways are involved [70–72].

The effect of heme combined with inflammatory stimuli such as LPS has been intriguing in different experimental models. Heme and LPS both act on TLR4 but at different sites [15]. In vitro studies in mice have demonstrated synergy in lethality and inflammation on combined heme and LPS exposure [73]. In a study with mice derived macrophages it was noted that heme and LPS synergy was enhanced in the presence of serum proteins at critical concentrations [74]. Interestingly, a recent publication showed the response of combined heme and LPS treatment varies in humans and mice macrophages. In human macrophages the combination reduced the inflammatory response while in mice macrophages it amplified the inflammatory response [75]. We did not find any evidence of increase or decrease in inflammatory response on combining heme and LPS in the PCLS model.

In line with our model, we found raised levels of inflammatory cytokines such as IL-6, IL-8, GDF15, CXCL1, CXCL2 and ferritin in serum of patients with COVID-19 in accordance with other published studies [51, 52, 76, 77]. Interestingly, 7 markers that were raised in serum of patients with COVID-19 and ARDS patients

such as IL-6, IL-8, HO-1, ferritin, CXCL1, CXCL2 and GDF-15 were also upregulated at gene and protein analysis of the heme-stimulated PCLS model, underlining the clinical relevance of our model. *In-vivo* chemokines such as CXCL2 [78], IL-8 [79], and TNF [80] caused chemotaxis of neutrophils from the circulation. While inflammatory cytokines such as IL-6, TNF and IL-1 $\beta$  cause haematopoiesis [81], raised GDF-15, has anti-inflammatory properties and raised levels in COVID-19 patients were associated with poor prognosis [76]. An additional mechanism that accentuates inflammation is ECM degradation by induced chemokines, cytokines, growth factors and adhesion molecules that leads to inflammation and injury [24].

In early phase of ARDS inflammation and ECM degradation occur [24]. Interestingly, we also observed effects on ECM expression after heme-induced injury in PCLS. We noted downregulations of genes that code for components of ECM such as collagen (*COL1A1*, *COL5A1*, *COL6A5*, *COL6A6*, *COL10A1*, *COL14A1*), elastin (*ELN*), laminin (*LAMB1*) and fibulin (*FBLN1*, *FBLN2*). Complementary to the loss of expression in ECM components, our dataset showed upregulation of proteinase genes such as matrix metalloproteinase (*MMP1,10,13,25*) and a disintegrin and metalloproteinase with thrombospondin motifs 4 (*ADAMTS4*). Clinical studies in ARDS patients showed raised MMP1 level which also indicates disease severity [82]. ADAMTS4 levels were raised in endotracheal aspirates in patients with ARDS due to severe influenza [83]. The transcriptomic and proteomic analysis identified upregulation MMP1 and ADAMTS4 in the heme-stimulated group, again emphasising the clinical application of our model. However, in later stages of ARDS fibroblasts are recruited which causes excess ECM deposition. ECM deposition may lead to post ARDS sequelae and fibrosis, which was extensively studied in COVID-19 survivors [84].

There is a lack of research investigating the mechanism of ARDS in human PCLS model [85, 86] and animal derived PCLS model [87]. The merit of our study is that our findings and the development of a new model for acute lung injury allows further mechanistic research and evaluation of pathways activated upon lung injury. To our knowledge, this study is the first to utilise transcriptomic and proteomics analysis in conjunction with the PCLS model to study heme-induced injury. The proposed model reduces need for animal studies in acute lung injury and ARDS research, supporting the 3 R (refine, reduce and replace) approach. However, we acknowledge the limitations of our study and our proposed model. The PCLS does not allow the study and recruitment of circulating inflammatory cells [31], which is important

during ARDS. Circulatory inflammatory cells such as neutrophils play a critical role in pathogenesis and disease progression of ARDS [88]. Most inflammatory signals that were detected in our experiments come from all the cell types present in the PCLS, immune cells along with structural cells such as epithelial cells, endothelial cells and fibroblasts. In addition, in patients in vivo heme enters the alveolus from the endothelial side or the site of trauma [89]. This injury side is not entirely comparable between ARDS patients and our experimental setting with heme being applied on tissue sections. Of note, PCLS also contain pulmonary vessels and heme affects these endothelial cells, which are known to be of greatest risk of heme exposure in vivo. Moreover, our PCLS model does not take into account the ventilatory stretch during respiration [31] and following mechanical ventilation in ARDS patients nor hypoxemic conditions. Additionally, the markers observed at the proteomic level were less than at the gene level. However, studies that have looked at transcriptomic and proteomic analysis observed that the protein expression is usually lower than RNA expression potentially due to post translational regulation or modification of instable proteins as compared to RNA or technical bias [90]. Despite washing with DPBS the possibility of residual heme from RBCs cannot be eliminated, but since the inflammatory response in heme-stimulated PCLS was compared to control PCLS from the same donor, which could also contain traces of heme, any contribution of heme from RBCs should have been adjusted. Though PCLS is a useful model it cannot fully replicate the complex pathogenesis of ARDS where during the disease course the triggers can amplify. The disease progression is additionally influenced by ARDS related factors such as hypoxia, hyperoxia, and cytokine increase that also affect lung response. Also, the PCLS were generated from some human donors with smoking history or tumor diagnosis, which might have primed lung tissue towards inflammatory stimuli which needs to be acknowledged as a limitation. For ethical reasons it is extremely difficult to obtain completely healthy lung tissue. A comparison to true healthy lung tissue is thus unfortunately not possible.

We aimed to establish heme stimulated PCLS as a novel model for acute lung injury and ARDS research. Although our model is limited to heme-stimulated injury, the model allows evaluation of involved mechanisms and testing of potential drug targets in ARDS. PCLS can be applied for testing the effectiveness of therapeutics prior to clinical testing. In our PCLS model, we have confirmed the findings of individual studies studying the effect of

heme in vitro [14, 27, 69]. We have also noted changes in ECM in lung injury, which have not been extensively studied during early stage of lung injury. The NF- $\kappa$  B and NLRP3 pathways are the main pathways involved in heme mediated inflammation. Heme induces lytic cell death caused by damage to membrane integrity. Targeted therapies towards these mechanisms may help improve the outcome of patients with ARDS. This approach of studying diseases from patient derived samples is a very valuable step towards advancement in personalised medicine as they point towards the pathological mechanism in diseased individuals and aid in planning targeted interventions.

## Conclusions

Heme induces inflammatory cytokines and cell death in human PCLS, similar to findings from patients with COVID-19 and ARDS. PCLS proved to be a useful translational tool to understand mechanism of action and disease pathophysiology, which might lead to discovery of novel targets and therapies. Further validation of the non-apoptotic cell death needs to be addressed in the future.

## Abbreviations

ADAMTS4	A disintegrin and metalloproteinase with thrombospondin motifs 4
ADJ	Adjusted
ARDS	Acute respiratory distress syndrome
BAL	Bronchoalveolar lavage
BP	Biological processes
CC	Cellular components
COPD	Chronic obstructive pulmonary disease
COVID-19	Coronavirus disease 2019
CXCL	C-X-C motif chemokine ligand
DEG	Differentially expressed genes
DEP	Differentially expressed protein
DPBS	Dulbecco's phosphate buffered saline
ECM	Extracellular matrix
ELN	Elastin
FBLN	Fibulin
GDF15	Growth differentiation factor
GESA	Gene set enrichment analysis
GO	Gene ontology
HO	Heme oxygenase
IC50	Half-maximal inhibitory concentration
IL-1 $\beta$	Interleukin-1 beta
IL-6	Interleukin 6
IL-8	Interleukin 8
KEGG	Kyoto encyclopedia of genes and genomes
LPS	Lipopolysaccharide
MMP	Matrix metalloproteinase
MP	Molecular processes
NLRP3	NOD like receptor protein 3
NOD	Nucleotide-binding and oligomerization domain
NF- $\kappa$ B	Nuclear factor $\kappa$ B
PCLS	Precision cut lung slices
RBC	Red blood cell
TLR	Toll like receptor
TNF	Tumour necrosis factor

## Supplementary Information

The online version contains supplementary material available at <https://doi.org/10.1186/s12931-025-03191-z>.

Supplementary Material 1. Table S1: Excel sheet has a list of DEG with log<sub>2</sub> FC and adj p-values from the transcriptomic analysis.

Supplementary Material 2: Table S2: Excel sheet has a list of DEP with log<sub>2</sub> FC and adj p-values from the proteomic analysis.

Supplementary Material 3.

### Acknowledgements

The authors would like to acknowledge Dr. John Stegmayr and Dr. Prof. Darcy Wagner for helping us optimise our RNA isolation protocol. Bulk RNA-sequencing was performed at the Next Generation Sequencing Platform of the University of Bern. Data analysis for transcriptomics was supported by the "Interfaculty Bioinformatics Unit (IBU) and Swiss Institute of Bioinformatics (SIB), University of Bern, Bern, Switzerland". Proteome analysis of protein lysates and data analysis was performed at the Core Facility Proteomics & Mass Spectrometry of the University of Bern. The authors acknowledge Prof. Martin Stämpfli and Dr Fabian Käsermann, who have supported this work.

### Author contributions

MFC, NK, KF, and CM designed the study. NK developed and performed the experiments. MFC, NK, CM, KF, CvG, TMM, PD contributed to sample and data collection. NK, CM, SC, JBP, CZ contributed to data acquisition. NK and CM analysed the data. NK, CM, KF and MFC interpreted the data. All authors revised the manuscript and approved the submitted version.

### Funding

This project has been funded by CSL Behring, Research, CSL Biologics Research Center, Bern, Switzerland. CSL representatives (KF, CZ, JBP and SC) contributed to study design and conduct.

### Availability of data and materials

No datasets were generated or analysed during the current study.

### Declarations

#### Ethics approval and consent to participate

The local Ethics Committee, Bern, Switzerland (KEK-BE\_2018-01801), approved the lung tissue sampling. COVID-19 participants signed a consent form before inclusion in the study that was approved by the local ethical committee (KEK 2020-00799). Blood was collected from 10 healthy volunteers after approval from Swiss ethical committee Bern (KEK\_246/15 PB\_2016-01524).

#### Consent for publication

Not applicable.

#### Clinical trial number

Not applicable.

#### Competing interest

The authors declare no competing interests.

#### Author details

<sup>1</sup>Department for Pulmonary Medicine, Allergology and Clinical Immunology, Inselspital, Bern University Hospital, University of Bern, Bern, Switzerland. <sup>2</sup>Lung Precision Medicine (LPM), Department for BioMedical Research (DBMR), University of Bern, Bern, Switzerland. <sup>3</sup>Department of General Thoracic Surgery, Inselspital, Bern University Hospital, Bern, Switzerland. <sup>4</sup>Department for BioMedical Research, University of Bern, Bern, Switzerland. <sup>5</sup>CSL Behring, Research, CSL Biologics Research Center, Bern, Switzerland. <sup>6</sup>Division of Pulmonology, Department of Medicine, Lausanne University Hospital (CHUV) and University of Lausanne, 1011 Lausanne, Switzerland.

Received: 14 November 2024 Accepted: 11 March 2025

Published online: 02 April 2025

## References

- Matthay MA, Arabi Y, Arroliga AC, Bernard G, Bersten AD, Brochard LJ, et al. A new global definition of acute respiratory distress syndrome. *Am J Respir Crit Care Med*. 2024;209(1):37–47.
- Bos LDJ, Ware LB. Acute respiratory distress syndrome: causes, pathophysiology, and phenotypes. *Lancet*. 2022;400(10358):1145–56.
- Kim WY, Hong SB. Sepsis and acute respiratory distress syndrome: recent update. *Tuberc Respir Dis (Seoul)*. 2016;79(2):53–7.
- Korkmaz FT, Traber KE. Innate immune responses in pneumonia. *Pneumonia*. 2023;15(1):4.
- World Health Organization 2023 data.who.int, WHO Coronavirus (COVID-19) dashboard > Deaths [Dashboard]. WHO; [<https://data.who.int/dashboards/covid19/deaths>].
- Sysiak-Sławecka J, Wichowska O, Piwowarczyk P, Borys M. The impact of bacterial superinfections on the outcome of critically ill patients with COVID-19 associated acute respiratory distress syndrome (ARDS)—a single-centre, observational cohort study. *Anaesthesiol Intensive Ther*. 2023;55(3):163–7.
- Bellani G, Laffey JG, Pham T, Fan E, Brochard L, Esteban A, et al. Epidemiology, patterns of care, and mortality for patients with acute respiratory distress syndrome in intensive care units in 50 countries. *JAMA*. 2016;315(8):788–800.
- Battaglini D, Fazzini B, Silva PL, Cruz FF, Ball L, Robba C, et al. Challenges in ARDS definition, management, and identification of effective personalized therapies. *J Clin Med*. 2023;12(4):1381.
- Bos LD, Schouten LR, van Vught LA, Wiewel MA, Ong DSY, Cremer O, et al. Identification and validation of distinct biological phenotypes in patients with acute respiratory distress syndrome by cluster analysis. *Thorax*. 2017;72(10):876–83.
- Calfee CS, Delucchi K, Parsons PE, Thompson BT, Ware LB, Matthay MA, et al. Subphenotypes in acute respiratory distress syndrome: latent class analysis of data from two randomised controlled trials. *Lancet Respir Med*. 2014;2(8):611–20.
- Janz DR, Bastarache JA, Peterson JF, Sills G, Wickersham N, May AK, et al. Association between cell-free hemoglobin, acetaminophen, and mortality in patients with sepsis: an observational study. *Crit Care Med*. 2013;41(3):784–90.
- Kempe DS, Akel A, Lang PA, Hermle T, Biswas R, Muresanu J, et al. Suicidal erythrocyte death in sepsis. *J Mol Med (Berl)*. 2007;85(3):273–81.
- Winslow R. HEMOGLOBIN. In: Laurent GJ, Shapiro SD, editors. *Encyclopedia of respiratory medicine*. Oxford: Academic Press; 2006. p. 263–7.
- Dutra FF, Alves LS, Rodrigues D, Fernandez PL, de Oliveira RB, Golenbock DT, et al. Hemolysis-induced lethality involves inflammasome activation by heme. *Proc Natl Acad Sci USA*. 2014;111(39):E4110–8.
- Figueiredo RT, Fernandez PL, Mourao-Sa DS, Porto BN, Dutra FF, Alves LS, et al. Characterization of heme as activator of Toll-like receptor 4. *J Biol Chem*. 2007;282(28):20221–9.
- Shaver CM, Upchurch CP, Janz DR, Grove BS, Putz ND, Wickersham NE, et al. Cell-free hemoglobin: a novel mediator of acute lung injury. *Am J Physiol Lung Cell Mol Physiol*. 2016;310(6):L532–41.
- Chen HY, Tzeng IS, Tsai KW, Wu YK, Cheng CF, Lu KC, et al. Association between heme oxygenase one and sepsis development in patients with moderate-to-critical COVID-19: a single-center, retrospective observational study. *Eur J Med Res*. 2022;27(1):275.
- Ekregbesi P, Shankar-Hari M, Bottomley C, Riley EM, Mooney JP. Relationship between anaemia, haemolysis, inflammation and haem oxygenase-1 at admission with sepsis: a pilot study. *Sci Rep*. 2018;8(1):11198.
- Mumby S, Upton RL, Chen Y, Stanford SJ, Quinlan GJ, Nicholson AG, et al. Lung heme oxygenase-1 is elevated in acute respiratory distress syndrome. *Crit Care Med*. 2004;32(5):1130–5.
- Ghio AJ, Carter JD, Richards JH, Richer LD, Grissom CK, Elstad MR. Iron and iron-related proteins in the lower respiratory tract of patients with acute respiratory distress syndrome. *Crit Care Med*. 2003;31(2):395–400.
- Abraham NG, Kappas A. Pharmacological and clinical aspects of heme oxygenase. *Pharmacol Rev*. 2008;60(1):79–127.
- Nagasawa R, Hara Y, Murohashi K, Aoki A, Kobayashi N, Takagi S, et al. Serum heme oxygenase-1 measurement is useful for evaluating disease activity and outcomes in patients with acute respiratory distress syndrome and acute exacerbation of interstitial lung disease. *BMC Pulm Med*. 2020;20(1):310.

23. Hara Y, Shinkai M, Taguri M, Nagai K, Hashimoto S, Kaneko T. ELISA development for serum hemoxygenase-1 and its application to patients with acute respiratory distress syndrome. *Can Respir J*. 2018;2018:9627420.
24. Ito JT, Lourenco JD, Righetti RF, Tiberio I, Prado CM, Lopes F. Extracellular matrix component remodeling in respiratory diseases: what has been found in clinical and experimental studies? *Cells*. 2019;8(4):342.
25. Wu Q, Pennini ME, Bergmann JN, Kozak ML, Herring K, Sciarretta KL, et al. Applying lessons learned from COVID-19 therapeutic trials to improve future ALI/ARDS trials. *Open Forum Infect Diseases*. 2022;9(8).
26. Porto BN, Alves LS, Fernandez PL, Dutra TP, Figueiredo RT, Graca-Souza AV, et al. Heme induces neutrophil migration and reactive oxygen species generation through signaling pathways characteristic of chemotactic receptors. *J Biol Chem*. 2007;282(33):24430–6.
27. Erdei J, Tóth A, Balogh E, Nyakundi BB, Bányaí E, Ryffel B, et al. Induction of NLRP3 inflammasome activation by heme in human endothelial cells. *Oxid Med Cell Longev*. 2018;2018:4310816.
28. Aggarwal S, Lam A, Bolisetty S, Carlisle MA, Traylor A, Agarwal A, et al. Heme attenuation ameliorates irritant gas inhalation-induced acute lung injury. *Antioxid Redox Signal*. 2016;24(2):99–112.
29. Aggarwal S, Jilling T, Doran S, Ahmad I, Eagen JE, Gu S, et al. Phosgene inhalation causes hemolysis and acute lung injury. *Toxicol Lett*. 2019;312:204–13.
30. Alsafadi HN, Uhl FE, Pineda RH, Bailey KE, Rojas M, Wagner DE, et al. Applications and approaches for three-dimensional precision-cut lung slices. *Disease modeling and drug discovery*. *Am J Respir Cell Mol Biol*. 2020;62(6):681–91.
31. Lehmann M, Krishnan R, Sucre J, Kulkarni HS, Pineda RH, Anderson C, et al. Precision cut lung slices: emerging tools for preclinical and translational lung research. *Am J Respir Cell Mol Biol*. 2024.
32. Liu G, Betts C, Cunoosamy DM, Aberg PM, Hornberg JJ, Sivars KB, et al. Use of precision cut lung slices as a translational model for the study of lung biology. *Respir Res*. 2019;20(1):162.
33. Guler SA, Machahua C, Geiser TK, Kocher G, Marti TM, Tan B, et al. Dehydroepiandrosterone in fibrotic interstitial lung disease: a translational study. *Respir Res*. 2022;23(1):149.
34. Stegmayr J, Alsafadi HN, Langwinski W, Niroomand A, Lindstedt S, Leigh ND, et al. Isolation of high-yield and -quality RNA from human precision-cut lung slices for RNA-sequencing and computational integration with larger patient cohorts. *Am J Physiol Lung Cell Mol Physiol*. 2021;320(2):L232–40.
35. Andrews S. A Quality Control Tool for High Throughput Sequence Data 2022. Available from: <http://www.bioinformatics.babraham.ac.uk/projects/fastqc/>.
36. Wang L, Wang S, Li W. RSeQC: quality control of RNA-seq experiments. *Bioinformatics*. 2012;28(16):2184–5.
37. Kim D, Langmead B, Salzberg SL. HISAT: a fast spliced aligner with low memory requirements. *Nat Methods*. 2015;12(4):357–60.
38. Liao Y, Smyth GK, Shi W. featureCounts: an efficient general purpose program for assigning sequence reads to genomic features. *Bioinformatics*. 2014;30(7):923–30.
39. Love MI, Huber W, Anders S. Moderated estimation of fold change and dispersion for RNA-seq data with DESeq2. *Genome Biol*. 2014;15(12):550.
40. Wu T, Hu E, Xu S, Chen M, Guo P, Dai Z, et al. clusterProfiler 4.0: a universal enrichment tool for interpreting omics data. *Innovation Camb*. 2021;2(3):100141.
41. Subramanian A, Tamayo P, Mootha VK, Mukherjee S, Ebert BL, Gillette MA, et al. Gene set enrichment analysis: a knowledge-based approach for interpreting genome-wide expression profiles. *Proc Natl Acad Sci USA*. 2005;102(43):15545–50.
42. Kanehisa M, Sato Y, Kawashima M. KEGG mapping tools for uncovering hidden features in biological data. *Protein Sci*. 2022;31(1):47–53.
43. Chang W, Joe Cheng J, Allaire J, Sievert C, Schloerke B, Xie Y, Allen J, McPherson J, Dipert A, Borges B. Shiny: Web Application Framework for R 2022. Available from: <https://CRAN.R-project.org/package=shiny>.
44. Yu F, Haynes SE, Teo GC, Avtonomov DM, Polasky DA, Nesvizhskii AI. Fast quantitative analysis of timsTOF PASEF data with MSFragger and IonQuant. *Mol Cell Proteomics*. 2020;19(9):1575–85.
45. Consortium TU. UniProt: a worldwide hub of protein knowledge. *Nucleic Acids Res*. 2018;47(D1):D506–15.
46. Strimmer K. A unified approach to false discovery rate estimation. *BMC Bioinformatics*. 2008;9:303.
47. Uldry AC, Maciel-Dominguez A, Jornod M, Buchs N, Braga-Lagache S, Brodard J, et al. Effect of sample transportation on the proteome of human circulating blood extracellular vesicles. *Int J Mol Sci*. 2022;23(9):4515.
48. Tyanova S, Temu T, Sinitcyn P, Carlson A, Hein MY, Geiger T, et al. The Perseus computational platform for comprehensive analysis of (prote)omics data. *Nat Methods*. 2016;13(9):731–40.
49. Szklarczyk D, Kirsch R, Koutrouli M, Nastou K, Mehryary F, Hachilif R, et al. The STRING database in 2023: protein–protein association networks and functional enrichment analyses for any sequenced genome of interest. *Nucleic Acids Res*. 2023;51(D1):D638–46.
50. Agrawal A, Balci H, Hanspers K, Coort SL, Martens M, Slenker DN, et al. WikiPathways 2024: next generation pathway database. *Nucleic Acids Res*. 2023;52(D1):D679–89.
51. McElvaney OJ, McEvoy NL, McElvaney OF, Carroll TP, Murphy MP, Dunlea DM, et al. Characterization of the inflammatory response to severe COVID-19 illness. *Am J Respir Crit Care Med*. 2020;202(6):812–21.
52. Khalil BA, Elemam NM, Maghazachi AA. Chemokines and chemokine receptors during COVID-19 infection. *Comput Struct Biotechnol J*. 2021;19:976–88.
53. Su WL, Lin CP, Hang HC, Wu PS, Cheng CF, Chao YC. Desaturation and heme elevation during COVID-19 infection: a potential prognostic factor of heme oxygenase-1. *J Microbiol Immunol Infect*. 2021;54(1):113–6.
54. Connelly KG, Moss M, Parsons PE, Moore EE, Moore FA, Giclas PC, et al. Serum ferritin as a predictor of the acute respiratory distress syndrome. *Am J Respir Crit Care Med*. 1997;155(1):21–5.
55. Sharkey RA, Donnelly SC, Connelly KG, Robertson CE, Haslett C, Repine JE. Initial serum ferritin levels in patients with multiple trauma and the subsequent development of acute respiratory distress syndrome. *Am J Respir Crit Care Med*. 1999;159(5 Pt 1):1506–9.
56. Mehta P, Samanta RJ, Wick K, Coll RC, Mawhinney T, McAleavey PG, et al. Elevated ferritin, mediated by IL-18 is associated with systemic inflammation and mortality in acute respiratory distress syndrome (ARDS). *Thorax*. 2024;79(3):227–35.
57. Petho D, Hendrik Z, Nagy A, Beke L, Patsalos A, Nagy L, et al. Heme cytotoxicity is the consequence of endoplasmic reticulum stress in atherosclerotic plaque progression. *Sci Rep*. 2021;11(1):10435.
58. Petrillo S, Chiabrando D, Genova T, Fiorito V, Ingoglia G, Vinchi F, et al. Heme accumulation in endothelial cells impairs angiogenesis by triggering paraptosis. *Cell Death Differ*. 2018;25(3):573–88.
59. Ryter SW, Tyrrell RM. The heme synthesis and degradation pathways: role in oxidant sensitivity. Heme oxygenase has both pro- and antioxidant properties. *Free Radic Biol Med*. 2000;28(2):289–309.
60. Lee SH, Shin JH, Park MW, Kim J, Chung KS, Na S, et al. Impairment of mitochondrial ATP synthesis induces RIPK3-dependent necroptosis in lung epithelial cells during lung injury by lung inflammation. *Immune Netw*. 2022;22(2):e18.
61. Qiu B, Zandkarimi F, Saqi A, Castagna C, Tan H, Sekulic M, et al. Fatal COVID-19 pulmonary disease involves ferroptosis. *Nat Commun*. 2024;15(1):3816.
62. Fortes GB, Alves LS, de Oliveira R, Dutra FF, Rodrigues D, Fernandez PL, et al. Heme induces programmed necrosis on macrophages through autocrine TNF and ROS production. *Blood*. 2012;119(10):2368–75.
63. Dang D, Meng Z, Zhang C, Li Z, Wei J, Wu H. Heme induces intestinal epithelial cell ferroptosis via mitochondrial dysfunction in transfusion-associated necrotizing enterocolitis. *FASEB J*. 2022;36(12):e22649.
64. Oeckinghaus A, Ghosh S. The NF-kappaB family of transcription factors and its regulation. *Cold Spring Harb Perspect Biol*. 2009;1(4):a000034.
65. Iyer SS, Pulsikens WP, Sadler JJ, Butter LM, Teske GJ, Ulland TK, et al. Necrotic cells trigger a sterile inflammatory response through the Nlrp3 inflammasome. *Proc Natl Acad Sci USA*. 2009;106(48):20388–93.
66. Franchi L, Eigenbrod T, Munoz-Planillo R, Nunez G. The inflammasome: a caspase-1-activation platform that regulates immune responses and disease pathogenesis. *Nat Immunol*. 2009;10(3):241–7.
67. Li H, Ambade A, Re F. Cutting edge: necrosis activates the NLRP3 inflammasome. *J Immunol*. 2009;183(3):1528–32.
68. Ghosh S, Adisa OA, Chappa P, Tan F, Jackson KA, Archer DR, et al. Extracellular heme crisis triggers acute chest syndrome in sickle mice. *J Clin Invest*. 2013;123(11):4809–20.

69. Belcher JD, Chen C, Nguyen J, Milbauer L, Abdulla F, Alayash AI, et al. Heme triggers TLR4 signaling leading to endothelial cell activation and vaso-occlusion in murine sickle cell disease. *Blood*. 2014;123(3):377–90.
70. Attiq A, Yao LJ, Afzal S, Khan MA. The triumvirate of NF-kappaB, inflammation and cytokine storm in COVID-19. *Int Immunopharmacol*. 2021;101(Pt B): 108255.
71. Millar MW, Fazal F, Rahman A. Therapeutic targeting of NF-kappaB in acute lung injury: a double-edged sword. *Cells*. 2022;11(20):3317.
72. Li W, Li D, Chen Y, Abudou H, Wang H, Cai J, et al. Classic signaling pathways in alveolar injury and repair involved in sepsis-induced ALI/ARDS: new research progress and prospect. *Dis Markers*. 2022;2022:6362344.
73. Fernandez PL, Dutra FF, Alves L, Figueiredo RT, Mourão-Sa D, Fortes GB, et al. Heme amplifies the innate immune response to microbial molecules through spleen tyrosine kinase (Syk)-dependent reactive oxygen species generation. *J Biol Chem*. 2010;285(43):32844–51.
74. Silva RCMC, Tan LB, Gama AMDS, De Cicco NNT, Merle NS, Roumenina LT, et al. Hemopexin and albumin inhibit heme-induced macrophage activation while also enabling heme-LPS synergistic promotion of TNF production. *Adv Redox Res*. 2023;8: 100069.
75. Pradhan P, Vijayan V, Liu B, Martinez-Delgado B, Matamala N, Nikolin C, et al. Distinct metabolic responses to heme in inflammatory human and mouse macrophages—role of nitric oxide. *Redox Biol*. 2024;73: 103191.
76. Alserawan L, Peñacoba P, Orozco Echevarría SE, Castillo D, Ortiz E, Martínez-Martínez L, et al. Growth differentiation factor 15 (GDF-15): a novel biomarker associated with poorer respiratory function in COVID-19. *Diagnostics*. 2021;11(11):1998.
77. Kurian SJ, Mathews SP, Paul A, Viswam SK, Kaniyoor Nagri S, Miraj SS, et al. Association of serum ferritin with severity and clinical outcome in COVID-19 patients: an observational study in a tertiary healthcare facility. *Clin Epidemiol Glob Health*. 2023;21: 101295.
78. Metzemaekers M, Gouwy M, Proost P. Neutrophil chemoattractant receptors in health and disease: double-edged swords. *Cell Mol Immunol*. 2020;17(5):433–50.
79. Henkels KM, Frondorf K, Gonzalez-Mejia ME, Doseff AL, Gomez-Cambronero J. IL-8-induced neutrophil chemotaxis is mediated by Janus kinase 3 (JAK3). *FEBS Lett*. 2011;585(1):159–66.
80. Peterson JM, Feedback KD, Baas JH, Pizza FX. Tumor necrosis factor- $\alpha$  promotes the accumulation of neutrophils and macrophages in skeletal muscle. *J Appl Physiol*. 2006;101(5):1394–9.
81. Caiado F, Pietras EM, Manz MG. Inflammation as a regulator of hematopoietic stem cell function in disease, aging, and clonal selection. *J Exp Med*. 2021;218(7).
82. Fligiel SE, Standiford T, Fligiel HM, Tashkin D, Strieter RM, Warner RL, et al. Matrix metalloproteinases and matrix metalloproteinase inhibitors in acute lung injury. *Hum Pathol*. 2006;37(4):422–30.
83. Boyd DF, Allen EK, Randolph AG, Guo XJ, Weng Y, Sanders CJ, et al. Exuberant fibroblast activity compromises lung function via ADAMTS4. *Nature*. 2020;587(7834):466–71.
84. Kewalramani N, Heenan KM, McKeegan D, Chaudhuri N. Post-COVID interstitial lung disease—the tip of the iceberg. *Immunol Allergy Clin North Am*. 2023;43(2):389–410.
85. Dutra Silva J, Su Y, Calfee CS, Delucchi KL, Weiss D, McAuley DF, et al. Mesenchymal stromal cell extracellular vesicles rescue mitochondrial dysfunction and improve barrier integrity in clinically relevant models of ARDS. *Eur Respir J*. 2021;58(1):2002978.
86. Magnen M, You R, Rao AA, Davis RT, Rodriguez L, Bernard O, et al. Immediate myeloid depot for SARS-CoV-2 in the human lung. *Sci Adv*. 2024;10(31):eadm8836.
87. Kryvenko V, Alberro-Brage A, Fysikopoulos A, Wessendorf M, Tello K, Morty RE, et al. Clathrin-mediated albumin clearance in alveolar epithelial cells of murine precision-cut lung slices. *Int J Mol Sci*. 2023;24(3):2644.
88. Yang SC, Tsai YF, Pan YL, Hwang TL. Understanding the role of neutrophils in acute respiratory distress syndrome. *Biomed J*. 2021;44(4):439–46.
89. Lee GR, Gallo D, Alves de Souza RW, Tiwari-Heckler S, Cszimadia E, Harbison JD, et al. Trauma-induced heme release increases susceptibility to bacterial infection. *JCI Insight*. 2021;6(20).
90. Prabahar A, Zamora R, Barclay D, Yin J, Ramamoorthy M, Bagheri A, et al. Unraveling the complex relationship between mRNA and protein abundances: a machine learning-based approach for imputing protein levels from RNA-seq data. *NAR Genomics Bioinf*. 2024;6(1).

## Publisher's Note

Springer Nature remains neutral with regard to jurisdictional claims in published maps and institutional affiliations.